Published in final edited form as:
Neurobiol Dis. 2010 July ; 39(1): 85–97. doi:10.1016/j.nbd.2010.04.001.

Microglial ablation and lipopolysaccharide preconditioning affects pilocarpine-induced seizures in mice

Martine M. Mirrione[1,2], **Dorothy K. Konomos**[1], **Iordanis Gravanis**[1], **Stephen L. Dewey**[1,2,3], **Adriano Aguzzi**[4], **Frank L. Heppner**[4,5], and **Stella E. Tsirka**[1]

[1] Department of Pharmacological Sciences, Molecular and Cellular Pharmacology, Stony Brook University, Stony Brook, New York 11794 [2] Medical Department, Brookhaven National Laboratory, Upton, New York 11973 [3] Psychiatry Department, New York University, School of Medicine, New York, New York 10016 [4] Institute of Neuropathology, University Hospital Zurich, CH-8091 Zurich, Switzerland [5] Department of Neuropathology, Charité - Universitätsmedizin Berlin, D-10117 Berlin

Abstract

Activated microglia have been associated with neurodegeneration in patients and in animal models of Temporal Lobe Epilepsy (TLE), however their precise functions as neurotoxic or neuroprotective is a topic of significant investigation. To explore this, we examined the effects of pilocarpine induced seizures in transgenic mice where microglia/macrophages were conditionally ablated. We found that unilateral ablation of microglia from the dorsal hippocampus did not alter acute seizure sensitivity. However, when this procedure was coupled with lipopolysaccharide (LPS) preconditioning (1 mg/kg given 24 hours prior to acute seizure), we observed a significant pro-convulsant phenomenon. This effect was associated with lower metabolic activation in the ipsilateral hippocampus during acute seizures, and could be attributed to activity in the mossy fiber pathway. These findings reveal that preconditioning with LPS 24 hours prior to seizure induction may have a protective effect which is abolished by unilateral hippocampal microglia/macrophage ablation.

Keywords

Microglia; seizure; epilepsy; lipopolysaccharide; status epilepticus; glucose; metabolism; positron emission tomography; pilocarpine; inflammation; mouse; FDG; imaging; immune system

Introduction

Microglia activation constitutes a major mechanism of self-defense against brain injury, infection and disease. The role undertaken by activated microglia is complicated, since they have been implicated as both neuroprotective and neurotoxic (Schwartz et al., 2006; Streit et al., 1999). Extensive microglial activation (microgliosis) and reactive astrogliosis occur in the brain parenchyma of individuals with recurrent seizure episodes and in animal models of epilepsy (Beach et al., 1995; Drage et al., 2002). In the pilocarpine mouse seizure model,

Corresponding author: Stella E. Tsirka, PhD, Department of Pharmacological Sciences, Stony Brook University, NY 11794-8651, Tel: 631-444-3859, Fax: 631-444-3218, stella@pharm.stonybrook.edu.

The authors declare no competing financial interests.

microgliosis persists for at least 30 days following seizure induction and correlates with local neuronal death (Borges et al., 2003; Borges et al., 2006). Microglia in the hippocampus may contribute to the re-occurrence of spontaneous seizures that take place days after the original epileptic event (Coulter, 2001; Pierce et al., 2005) by facilitating aberrant migration of newborn neurons (Yang et al., 2009). Changes in glial function could perhaps be a component of metabolic abnormalities which are observed in epileptic patients (Altay et al., 2005; Lamusuo et al., 2001; Magistretti and Pellerin, 1996; Vielhaber et al., 2003) and rodent seizure models (Goffin et al., 2009; Kornblum et al., 2000; Mirrione et al., 2007; Mirrione et al., 2006). The question remains however, whether microgliosis is a consequence of recurrent seizure episodes, a bystander to neuronal damage, or if microglia could directly contribute to seizure symptoms, sensitivity, or threshold. One approach to investigate this question is to modulate the microglia activation state concurrently with seizures.

Recent studies have suggested that preconditioning microglia with bacterial lipopolysaccharide (LPS) can be protective in rodent seizure models (Akarsu et al., 2006; Arican et al., 2006; Dmowska et al., 2009; Sayyah et al., 2003b), a concept which has been critically investigated in ischemia (Marsh et al., 2009b; Rosenzweig et al., 2004). The mechanism of protection in ischemia has been shown to involve tumor necrosis factor alpha (TNF-α), interleukin-1 beta (IL-1β), and reprogramming of the cellular response to excitotoxic insults (Marsh et al., 2009a; Saha et al., 2009), but the potential for protection in epilepsy is controversial and less understood. In one study, LPS administration prior to pentylenetetrazole (PTZ)-induced seizures, was beneficial by increasing plasma levels of nitric oxide (NO) and interleukin-6 (IL-6), which reduced blood brain barrier (BBB) permeability (Arican et al., 2006). A time course of LPS delivery prior to seizure induction with PTZ demonstrated complex effects, where LPS administered 4 hrs before PTZ-induced seizures was pro-epileptic, but when given 18 hrs before, it conferred anticonvulsant effects attributable to the expression of cycloxygenases-1 (COX-1) and -2 (Akarsu et al., 2006). LPS was inhibitory in a kindling model of seizures but only when it was administered daily for 16 days (Sayyah et al., 2003b). Neuronal protection from cell death was observed after LPS preconditioning 72 hours prior to seizure induction (Dmowska et al., 2009). Several other studies have supported either no effect (Yuhas et al., 2002) or a pro-convulsant role for LPS when given 1–2 hours prior to seizures (Sankar et al., 2007; Sayyah et al., 2003a). It is clear from these studies that both positive and negative effects are induced by LPS that appear to be time and dose dependent, thus warranting further investigation. In the present study, we have focused on the effects of LPS when given 24 hours prior to piolocarpine injection, as in the protocol used by Akarsu and colleagues (2006), in order to explore the role of preconditioned microglia in seizure induction. This dose and timing of LPS administration did not result in promotion of seizures.

We previously showed that the threshold to experimentally induced seizures, and neuronal survival following intra-hippocampal kainate injections is affected by the levels of the protease tissue plasminogen activator (tPA) (Carroll et al., 1994; Mirrione et al., 2007; Tsirka et al., 1995; Wu et al., 2000; Zhang et al., 2005), which during excitiotoxic events, can activate microglia and exacerbate neuronal injury (Gravanis and Tsirka, 2004; Rogove et al., 1999; Siao and Tsirka, 2002). Based on this evidence, we hypothesized that microglial activation could influence the threshold and/or sensitivity to pilocarpine induced seizures and downstream pathology. To explore this, we evaluated microglia during acute seizures using a recently developed transgenic model of conditional microglia and macrophage ablation (Heppner et al., 2005). In these mice, administration of the prodrug gancyclovir (GCV) targets cells which express the herpes simplex virus thymidine kinase (HSVTK) suicide gene under the microglia/macrophage CD11b promoter, thereby causing specific ablation following DNA replication failure. We evaluated behavioral seizure symptoms, histology, and *in-vivo* metabolic activity (which measures brain activity on a systems level), following ablation of microglia/macrophages with and without LPS preconditioning. Our results demonstrate a significant

modulatory role for preconditioned hippocampal microglia in mitigating acute seizure induction.

Materials and Methods

Animals and genotyping

Transgenic animals expressing thymidine kinase (TK) in cells of monocytic lineage, including microglia and macrophages, were generated (CD11b-HSVTK+/−) (Heppner et al., 2005). C57Bl/6 wild-type (wt) males were bred with females heterozygous for the transgene (CD11b-HSVTK+/−) due to male sterility, and offspring were genotyped by PCR with Taq DNA polymerase in 17 mM $MgCl_2$ PCR buffer with the following primers: 5′-GACTTCCGTGGCTTCTTGCTGC-3′ and 5′-GTGCTGGCATTACAGGCGTGAG-3′. The PCR conditions were as follows: 95°C for 3 min, 34 cycles (95°C for 30 s, 60.5°C for 30s, 72° C for 45 s) 72°C for 4 min. Wild type littermates (that lacked the CD11b-HSVTK allele, hereafter referred to as CD11b-HSVTK−/−) were used as controls. All animal procedures were approved by the Institutional Animal Care and Use Committee (IACUC) at Stony Brook University and Brookhaven National Laboratory (BNL). Animals were housed individually on a 12:12 hour light: dark cycle with food ad libitum.

Surgical procedures

For chronic unilateral intrahippocampal infusion of gancyclovir (GCV), animals were anesthetized with an intraperitoneal injection of atropine (0.6 mg/kg), and 1.25% Avertin anesthesia (0.02 ml/g), and the site of infusion was determined using stereotactic coordinates (David Kopf Instruments, Tujunga, CA). Unilateral intracerebral administration of substances is routinely used in our lab, as it allows the contralateral side to function as an internal control, thus reducing the number of animals necessary to carry out the experiment. The coordinates from bregma were 2.5 mm posterior, and 1.7 mm lateral for pilocarpine experiments, or 0.5 mm lateral for kainite experiments. A guide cannula (Plastics One), pre-cut to 1.6 mm length was inserted. The guide cannula was connected via clear vinyl tubing (Plastics One) to mini osmotic pumps (Alzet®, DURECT Corporation), containing 100 μl of GCV at concentrations ranging between 0.75–2 mg/ml (Calbiochem). Pumps were incubated at 37°C for a minimum of 4 hrs in phosphate buffered saline (PBS). Each pump (infusion rate either 0.25 μl/hr over 14 days for pilocarpine experiments, or 0.5 μl/hr over 7 days for kainate experiments) was placed subcutaneously while the cannula was secured to the skull. Following surgery, animals were injected subcutaneously with the analgesic buprenorphine HCL (Bedford labs, Bedford, OH) (0.03mg/kg). At the end of the experimental period, pumps were evaluated to verify that the cannula flow was not blocked and that the drug was delivered to the correct location. The remaining drug volume was also determined to ensure efficient delivery.

Control vehicle infusions were previously evaluated using saline or PBS delivery via micro-osmotic pumps followed by excitotoxic injury or LPS stimulation or pilocarpine delivery. The control pump-infused animals were compared to non-injured control animals. The behavioral and histological outcomes were the same, with the only exception being the presence of a very confined area of microglial activation surrounding the site of cannula placement in the brain. No neuronal death or other cell activation was observed. Additionally, the experiments on kainate neurotoxicity provide an indication of how far gancyclovir diffuses (please see supplementary figure 1I showing microglial ablation to the CA3 region of the dorsal hippocampus diffused from the subiculum). This is consistent with the results we obtained (a diffusion point from the CA1 area spreading throughout the dorsal hippocampus to the DG and CA3). Areas of the ventral hippocampus in our experiments (more than 3 mm from the infusion site) showed normally activated microglia.

Intrahippocampal injection of kainate (KA)

Two days after GCV infusion onset, the mice were injected with KA. In brief, adult wild-type (CD11b-HSVTK−/−), or transgenic (CD11b-HSVTK+/−) mice weighing 20–25g were injected i.p. with atropine (0.6 mg/g of body weight) and deeply anesthetized with 1.25% Avertin (0.02 ml/g of body weight). At stereotaxic coordinates −2.5 mm from bregma and 1.7 mm lateral, a small burr hole was made. PBS or KA (Sigma) at 0.75 nmol was delivered in 300 nl PBS at a depth of 1.6 mm over 60sec, and the needle remained in place for an extra 2 min to prevent reflux. Five days after injection the mice were sacrificed, their brains removed and fixed overnight in 4% paraformaldehyde. Coronal sections (25 μm) through the hippocampus were stained with cresyl violet to quantify neuronal survival. The dose of KA used does not elicit any seizure activity in the animals.

Pilocarpine mouse seizure model

Seizures were induced using the acetylcholine receptor agonist pilocarpine hydrochloride (Sigma), as described previously (Mirrione et al., 2006; Schauwecker and Steward, 1997). Mice were injected first with methylscopolamine (2 mg/kg i.p. in 0.9% saline, Sigma) to minimize peripheral cholinergic effects, and 15–30 min later with pilocarpine hydrochloride (260 or 280 mg/kg i.p.). Seizures were recorded using a digital video camera coupled to a PC with Ulead Video Studio software (www.ulead.com). Seizure intensity was determined using a scale of 0–7; 0: normal activity; 1: immobility; 2: forelimb and/or tail extension, rigid posture; 3: repetitive movements, head bobbing; partial body clonus 4: rearing; 5: continuous rearing and falling, whole body clonus; 6: severe tonic-clonic seizures with loss of posture or jumping and 7: mortality (Borges et al., 2003; Racine et al., 1972; Schauwecker and Steward, 1997). The experimenter was blinded to genotype while scoring seizure intensity, which was then confirmed by a second independent observer. Status epilepticus (SE) was defined by continuous seizure activity for at least 30 minutes and included multiple stage 4–6 level seizures. Seizure symptoms were continuously monitored for 60 minutes, and the maximum score observed in 5-minute intervals was used to establish a mean overall seizure score for each animal. In the event of mortality, a score of 7 was denoted for the remainder of the observation period and factored into the overall score. Animals were monitored for an additional hour and then daily during the experiment for recovery. Mice were injected (i.p.) with 300 μl of 5% dextrose in Ringer's solution if weight loss was apparent.

Experimental groups

Group conditions are outlined in Table 1. Group I (n=3 CD11b-HSVTK−/− and n=3 CD11b-HSVTK+/−) mice were given pilocarpine at the dose 280 mg/kg. Group II (n=6 CD11b-HSVTK−/− and n=8 CD11b-HSVTK+/−) received mini osmotic pumps containing GCV (with 7 days of infusion) prior to 280 mg/kg pilocarpine induced seizures. For group III (n=3 CD11b-HSVTK−/− and n=3 CD11b-HSVTK+/−) animals were given a pre-treatment of lipopolysaccharide LPS (1 mg/kg) 24 hours prior tissue collection. Group IV animals (n=3 CD11b-HSVTK−/− and n=3 CD11b-HSVTK+/−) received LPS and pilocarpine (280 mg/kg) the following day. Group V (n=10 CD11b-HSVTK−/− and n=7 CD11b-HSVTK+/−) received GCV infusion, LPS pretreatment, and pilocarpine (280 mg/kg). Group VI (n=10 CD11b-HSVTK−/− and n=13 CD11b-HSVTK+/−) mice were given GCV infusion, LPS pre-treatment and a lower dose of piloarpine (260 mg/kg). Animals were pooled from 2 or 3 separate experiments for groups II, V, and VI. The overall seizure severity trend was consistent in all experiments.

Small animal PET

For small animal imaging a subset of animals from Group V were used: n=6 CD11b-HSVTK −/− and n=4 CD11b-HSVTK+/−, aged 2–3 months, 22–31 gr. These animals received a

maximum of 4 microPET scans (scan 1: naïve, scan 2: GCV pump baseline [allowing for 2 days of recovery between the surgery and the second scan], scan 3: GCV pump acute seizures, scan 4: GCV pump day 7 post seizures), one scan per week over consecutive weeks as previously described (Mirrione et al., 2006). For each scan, animals were injected i.p. with 500 μCi (200–500μL) of ^{18}FDG and returned to their home cage for a 60-min uptake period. Mice were anesthetized with atropine (0.6 mg/kg, i.p.) and 1.25% Avertin (0.02 ml/g, i.p.) and scanned using a 10-min acquisition protocol. Whole blood glucose was measured by collecting 10μl of tail vein blood using glucose strips and a glucometer (CVS brand). Following maximum-likelihood expectation maximization algorithm (MLEM) reconstruction, data were spatially preprocessed using PMOD (http://www.pmod.com) and Statistical Parametric Mapping (SPM2) software (http://www.fil.ion.ucl.ac.uk/spm), as previously described (Mirrione et al., 2007). In brief, the analysis design selected was 'PET multi-subject condition and covariate' for comparisons where each scan (1–4) was entered as a separate condition. Main effects were modeled by entering contrasts of 0, 1, or −1 for each condition depending on the comparison. This analysis determined differences between each pair of scans within groups and provided an overall 3-dimensional map (*T-map*) of the statistically significant voxels apparent between the conditions. Methylscopolamine alone did not alter ^{18}FDG uptake (Mirrione et al., 2007).

Tissue collection

Following acute seizures mice were sacrificed by 2 hours post pilocarpine injection, at day 3 by transcardial perfusion, or in the cases of mortality, fresh brain tissue was collected as soon as possible and placed in 4% paraformaldehyde (PFA). For perfusions, mice were anesthetized with an i.p. injection of Avertin and then rapidly transcardially perfused using PBS coupled with 100μl containing 1000units/ml of heparin, followed by 35–50ml of 4% PFA in PBS (pH 7.4). A subset of mice from group VI (n=4) were not perfused to maintain conditions for measuring tPA activity (see *zymography* below). Brains were rapidly excised, post fixed for an additional hour in 4% PFA, and then placed in 30% sucrose with 0.02% sodium azide at 4° C until fully dehydrated. Tissue was then frozen embedded in O.C.T. Compound (Tissue-Tek) overnight and sectioned using a Leica (Nussloch, Germany) cryostat into 14–30 μM coronal sections. Sections were mounted onto slides (Fisher SuperFrost Plus; Fisher Scientific), air dried, and stored at −80°C.

Immunohistochemistry

Slides were post fixed in 4% PFA/PBS for 20 min at room temperature and procedures were conducted according to previously established methods (Siao et al., 2003). For biotinylated secondary antibodies, endogenous peroxidase activity was quenched with peroxide treatment (3% H_2O_2 in PBS, or 0.3% H_2O_2 in methanol for 20–30min). Blocking was performed in serum from the host of the secondary antibody [5–10% serum in PBS-T (0.5% Triton X-100 in PBS)] for 1 hr at room temperature. Primary antibodies used at the following concentrations, Iba1 1:500 (Wako Pure Chemical Industries, Ltd), glial fibrillary acidic protein (GFAP) 1:1000 (Dako), and neuropeptide Y (NPY) 1:500 (Chemicon) were added into 3–5% serum in PBS-T overnight at 4°C. After washes in PBS, appropriate biotinylated or fluorescent secondary antibodies were added in serum/PBS-T and incubated for 1 hour at room temperature with agitation. For fluorescence microscopy, slides were mounted with VectaShield and DAPI. For biotinylated secondary antibodies, the ABC reagent was added to conjugate avidin-peroxidase to the immune complex (Vector Laboratories, Burlingame, CA). The signal was visualized using Fast 3,3′-Diaminobenzidine (DAB) Tablet Sets (Sigma). For isolectin B4 histological stain, sections were incubated with Bandeiras simplicifolia isolectin B4 conjugated to peroxidase (Sigma). After extensive washing, the signal was visualized with DAB. Select sections were counterstained with cresyl violet for neuronal survival/death, successively

dehydrated in ethanol, defatted in xylenes, and cover slipped with Permount (Fisher Scientific, Houston, TX).

Slides were photographed digitally using SPOT advanced software (www.diaginc.com/SpotSoftware/) on a Nikon Eclipse E600 microscope under bright-filed optics at 4× or 40×. For figures 1, 2 and 4 displaying Iba1+ microglia, images were taken from the CA1 and DG subregions at 2.3–2.7 mm from bregma. Coordinates for the CA1 images were taken centered at 1.6–1.8 mm medial and 1.8 mm ventral. Coordinates for the DG were from 1.4–1.7 mm medial and 1.7–1.9 mm ventral. Quantification of microglia was done by a blinded experimenter, by counting the total number of iba1 positive cells at 40× in a rectangular region of interest (300×400 μm^2). 2–3 fields were counted per animal and group counts were averaged; results are presented as means ± standard error of the mean (S.E.M) in the counted area.

Zymography for tPA proteolytic activity

Fresh frozen sections (30 μm) from 2 mice per genotype from group VI (with representative seizures scores per group, 1.1±0.1 for CD11b-HSVTK−/−, and 2.6±0.9 for CD11b-HSVTK+/−, average ± S.E.M.) were overlaid with an agarose mixture containing plasminogen, ammiloride, and 10% milk for 1–3 hours at 37°C as previously described (Siao and Tsirka, 2002). tPA activity was inferred by enzymatic clearing of the white substrate. Slides were observed with a Nikon Eclipse E600 microscope using dark field illumination. The mean area of clearing in the CA3 or DG over the total hippocampus was quantified (arbitrary units).

Statistical analyses

All statistics were performed using SPSS Statistics 17.0, GraphPad Prism 4.00 for Windows, GraphPad Software (http://www.graphpad.com), or Microsoft Excel. Numerical data were graphically presented using Prism. Univariate Analysis of Variance (ANOVA) was conducted between genotype and group for overall seizure score and further evaluated with Tukey honest significance post-tests for within group comparisons, or student t-tests for between group comparisons. Data from interval seizure scoring, Iba1 cell counts, and ROI analysis, are displayed as the mean ± S.E.M. and were analyzed by Two-way ANOVA with Bonferroni post-tests.

Results

Reduction of the extent of excitotoxic cell death in the absence of activated microglia

Experimental neuronal death in the hippocampus is accompanied by microglia/macrophage activation, an event that also contributes to the progression of cell death. We have previously shown that delay of microglia activation protects neurons from cell death (Rogove and Tsirka, 1998). As a proof of principle using transgenic microglia/macrophage ablation, we assessed if neuroprotection would be obtained in excitotoxin-challenged CD11b-HSVTK+/− mice. We delivered gancyclovir (GCV) unilaterally to the dorsal hippocampus, off midline, to spatially accommodate the subsequent injection of either kainic acid (KA) or PBS to the CA1 two days later. We have previously shown KA induces neuronal death as analyzed five days later, and it should be noted that the dose of KA used in this protocol does not induce any seizure activity (Tsirka et al., 1995; Tsirka et al., 1997; Rogove et al., 1999; Siao et al., 2003; Parathath et al., 2007; Sheehan et al., 2007).

As shown in Supplemental Figure 1, the delivery of GCV alone had no effect on the tissue nor did it elicit any microglial response (panels a-c), comparable to delivery of PBS alone (data not shown and (Sheehan et al., 2007). Following GCV infusion, injection of KA in wild-type animals (littermates lacking the transgene designated as CD11b-HSVTK−/−) showed typical

neuronal sensitivity to KA and microglial activation, migration and accumulation to the site of cell death (the CA1 subregion, indicated by arrows in panels D and E). However, GCV infusion and injection of KA in CD11b-HSVTK+/− animals (littermates containing the transgene *HSVTK* on one CD11b locus) resulted in protection to neurons from KA-induced death, and reduced both the number of detectable microglia and their activation state (panels E versus H, and the high magnification images F versus I). Iba1+ cell counts for each group in the CA1, CA3, and DG reveal group differences as shown in panel J (two-way ANOVA, Bonferroni post tests $p<0.001$). The small extent of CA3 cell death in G may have resulted from acute necrotic death ensuing from the KA injection, as the same area in I shows efficient diffusion of GCV to ablate microglia throughout the dorsal hippocampus. These results are consistent with our previous data using macrophage inhibitory factor (MIF) to inhibit microglia activation (Rogove and Tsirka, 1998), and demonstrate microglia activated consequent to excitotoxic neuronal death are functioning to phagocytose necrotic cellular debris.

Quiescent hippocampal microglia do not modulate seizure threshold

As the localized GCV delivery was effective in the excitotoxic paradigm, we investigated the hypothesis that activated microglia could modulate seizure induction threshold based on data from our lab and others (Beach et al., 1995; de Bock et al., 1996; Drage et al., 2002; Ravizza et al., 2008; Riazi et al., 2008; Rodgers et al., 2009; Shapiro et al., 2008; Turrin and Rivest, 2004; Yang et al., 2009). We used the transgenic microglia/macrophage ablation mouse model to investigate this question, and the pilocarpine paradigm of SE to elicit seizures and assess the effect of microglial elimination.

Figure 1 compares acute seizures with and without GCV infusions in CD11b-HSVTK−/− (wt) and +/− mice. Panel A outlines the group conditions for the experiment. Acute seizures were induced in group I and II using standard protocols (2mg/kg methylscopolamine followed by 280 mg/kg pilocarpine), however group II also received 7 days of GCV infusion unilaterally directly to the CA1 region of the hippocampus. Animals were observed for 60 minutes following pilocarpine injection where seizure symptoms were continuously recorded. Seizure activity was rated with the Racine Scale 0–6 (Racine et al., 1972), and a score of 7 was added to denote mortality. An overall seizure score was calculated by averaging the maximum scores during each 5 minute interval over the 60 min observation period (Figure 1B). No significant differences in seizure threshold were found between genotypes or groups with average scores being 3.67±0.76 (n=3), 4.88±0.66 (n=3) for group I and 2.86±0.53 (n=6), 3.43±0.62 (n=8) for group II, (−/−) and (+/−) respectively. To represent the data with more detail, we show interval scores for each genotype in group II over the observation period (Figure 1C), showing an onset to stage 3 seizures at 12.5±3.35min (−/−) or 9.2.0±2.4min (+/−), followed by a steady expression of stage 3–5 seizures. No statistically significant differences were found between genotypes.

Animals in each group were sacrificed within 2 hours following pilocarpine injection and evaluated for the presence of activated microglia (using immunofluorescence against Iba1) to assess the effectiveness of ablation. Figure 1D and E show representative sections with microglia/macrophages (green) and neuronal layers (nuclei stained for DAPI) in the CA1 and DG of the ipsilateral/injected hippocampus. Quantification of Iba1+ cells (counted per $300\times400\ \mu m^2$ region) is given to the right of each set of sections. No significant differences were found in the CA1 or DG between genotypes in group I with average scores being 64±4, 59±8 for CA1 and 38±4, 46±5 for DG, (−/−) and (+/−) respectively. In group II however, histology confirmed efficient microglia ablation in CD11b-HSVTK+/− mice, as we did find significant differences between genotypes in both the CA1 (63±3 > 20±5) and DG (42±10 > 11±1) regions, (CD11b-HSVTK−/− greater than CD11b-HSVTK+/−, tested with two-way ANOVA, Bonferroni post tests $p<0.05$). The arrows in Figure 1E indicate several activated

microglia/monocytes in the CA1 and DG of −/− mice, but only a few scattered, dystrophic Iba1 positive cells in +/− mice. It should be noted that the intensity of DAPI in panels D and E were different due to taking the pictures at different times, but do not reflect any change in neuronal density. Astrocytes were also evaluated with GFAP and found to be unaffected by microglia ablation (data not shown), consistent with (Falsig et al., 2008). Furthermore, microglia ablation was confined to the dorsal hippocampus of +/− mice, as normal microglial activation was observed in other regions such as the thalamus and frontal cortex (data not shown). Overall, these results suggested that the presence of quiescent hippocampal microglia per se does not inherently change the seizure induction threshold or acute seizure sensitivity in mice, although since our experimental design employed unilateral hippocampal ablation further studies are warranted to support this conclusion.

Activated microglia and LPS preconditioning modulate seizure threshold

Since previous studies have demonstrated an interaction between microglia preconditioning with lipopolysaccharide (LPS) and seizure threshold (Akarsu et al., 2006; Arican et al., 2006; Auvin et al., 2009; Dmowska et al., 2009; Sayyah et al., 2003a; Sayyah et al., 2003b), and since we were interested in determining if modulating microglia activation could influence seizure vulnerability, we exposed subsequent groups to an LPS pre-treatment following the same seizure induction paradigm. Based on evidence from the literature, we chose to administer LPS 24 hours prior to seizure induction (Akarsu et al., 2006; Sayyah et al., 2003a).

Figure 2A outlines the group conditions for the experiment. Group III received LPS only, group IV received LPS followed 24 hours later by pilocarpine induced seizures, and group V received 7 day of GCV infusion and LPS 24 hrs prior to pilocarpine (brain tissue was collected the day after LPS injection). Overall seizure scores shown in Figure 2B indicated normal behavior for group III (LPS, scores of zero, as expected; −/−, n=3 and +/−, n=3) and typical seizure activity in group IV (LPS+PILO) 2.69±0.56 (−/−, n=3) and 2.24±0.30 (+/−, n=3). We did observe however, a trend toward reduced seizure symptoms concurrent with LPS administration when comparing pilocarpine alone versus LPS pretreatment with pilocarpine (Univariate ANOVA, Tukey HSD post test, p=0.062).

Overall seizure scores for group V (GCV+LPS+PILO) revealed significant differences in seizure sensitivity between genotypes 2.14±0.35 (−/−, n=10), 4.35±0.50 (+/−, n=7), (p=0.002, *t*-test). The onset times to the first stage 3 seizure were at 20.56±4.52 min for −/−, and 15.0 ±1.5 min for +/− (Figure 2C). Furthermore, a significant divergence in scores emerged starting 25-min after pilocarpine injection (Two-way ANOVA, Bonferroni post-tests), as +/− mice showed more severe generalized seizures and increased rate of mortality (2 out of 10 or 20% for −/−, versus 6 out of 7 or 86% for +/−). In the graph presented, all intervals post death were scored at 7, making the divergent effect clearly obvious. However, it is important to note that even when the analysis was limited to include only one scoring point of ‘7’ (and then not include any scores for the subsequent time intervals up to 60 min), there was still a significant difference between the genotypes by two-way ANOVA ($p<0.0001$), and Bonferroni post-hoc comparisons at 25 min, 35 min ($p<0.01$) and 50 min ($p<0.05$) due to the increased number of stage 4–6 level seizures preceding mortality in +/− mice (data not shown).

Histological evaluation confirmed activation of microglia in all LPS treated groups, and cell counts did not reveal significant differences between genotypes in expression of Iba1+ cells by LPS or PILO alone (Figure 2D,E). However, the analysis did reveal significant differences in group V (wild type mice receiving GCV, LPS, and PILO versus similarly-treated transgenic mice; panel F) for the CA1 (43±8 > 9±3), and DG (39±7 > 10±2), (CD11b-HSVTK−/− greater than CD11b-HSVTK+/−, two-way ANOVA, $p<0.0001$, with Bonferroni post-tests).

Overall, these data suggest that hippocampal microglia can be significant modulators of the threshold of seizure induction. When hippocampal microglia were preconditioned with LPS 24 hours prior to pilocarpine injection, both genotypes of mice experienced lower acute seizure scores, although the difference was not statistically significant (compare group I verses IV, Figure 1B and Figure 2B). However, the ablation of LPS-preconditioned microglia resulted in significantly higher acute seizure scores in CD11b-HSVTK+/− mice (compare group II verses V, Figure 1B,C and Figure 2B,C). Further experiments are required to identify the chemical mediators underlying this phenomenon, and whether there would be an additive effect with bilateral micorglial ablation.

Metabolic correlates of seizures and microglia/macrophages in LPS preconditioned mice

We next explored the divergent seizure sensitivity observed in the group V (GCV+LPS+PILO) animals using metabolic imaging. We have previously shown correlations between seizures and region-specific ^{18}FDG uptake (Mirrione et al., 2007; Mirrione et al., 2006). We asked if these correlations would be altered by LPS preconditioning and microglia/macrophage ablation. Our goal was to identify the brain regions involved in this behavioral divergence using a systems approach.

A subset of animals from Group V (GCV+LPS+PILO, n=6 −/−, n=4 +/−) were used for the imaging experiments (Figure 3). Normal metabolic activity was confirmed in both genotypes with baseline scans where ^{18}FDG uptake was quantified in the naïve state (Scan 1: Baseline). The same mice were imaged again following recovery from GCV pump implantation (Scan 2: Baseline with GCV pump). A hypometabolic area in the ipsilateral cortex of each genotype was found corresponding to the cannula implantation site, which remained present throughout the course of the experiment (Figure 3A, 'Probe' two-way ANOVA, Bonferroni post-tests, ***, $p<0.001$ for both genotypes). This was in agreement with previous data showing metabolic decreases associated with probe implants in rats (Schiffer et al., 2006). Immunohistochemical analysis confirmed the presence of inflammatory response and tissue damage at the implantation site coincident with localized cortical hypometabolism (data not shown). No other differences were observed between genotypes or between scans 1 and 2.

One week later, LPS was administered and seizures were induced concurrently with ^{18}FDG injection. Metabolic imaging was preformed following a 60-minute uptake period during which time seizure symptoms were recorded (Scan 3: Pilocarpine). Interval scores for this subset of group V (GCV+LPS+PILO) are shown in Figure 3B (two way ANOVA, Bonferroni post-tests, **$p<0.01$, ***$p<0.001$). The overall scores were significantly different between genotypes; the average score for CD11b-HSVTK−/− animals was 1.88±0.19, whereas that of CD11b-HSVTK+/− animals was 4.68±0.63, ($p=0.002$, *t*-test). All mice underwent scanning, however between 35–70 min, mortality was observed in 1/6 (17%) of CD11b-HSVTK−/−, and 4/4 (100%) of CD11b-HSVTK+/− mice. Region of interest analysis revealed significant changes between scans 3, and scans 1 or 2. Specifically, a decrease in metabolic activity was observed in the striatum, and a significant increase in activity was found in the septum, hippocampus (left and right combined), thalamus, midbrain, and cerebellum (Figure 3A, and data not shown, *, $p < 0.05$, **$p<0.01$, ***$p<0.001$, two-way ANOVA, Bonferroni post-tests comparing all scans to each other by region).

A voxel based SPM analysis was employed to quantify regional changes in ^{18}FDG uptake with greater specificity, thus removing the constraint of pre-determined ROIs (maps show areas of statistically significant changes below a threshold *p* value set at 0.001 uncorrected, with the associated *t*-score given as a color range). A comparison of the main effect between scans 2 and 3 demonstrated increases in ^{18}FDG uptake corresponding to the septum, thalamus, hippocampus, midbrain, and cerebellum, and decreases in the striatum for both genotypes corresponding to the ROI analysis (Figure 3C, and data not shown). This pattern of pilocarpine-

induced activation was consistent with our previous findings in wild type mice (Mirrione et al., 2007). However in the current study, the analysis did show unilateral differences in hippocampal ^{18}FDG uptake between genotypes. Although CD11b-HSVTK+/− mice displayed more severe symptoms, there appeared to be a lack of ^{18}FDG uptake in the dorsal hippocampus around the site of GCV infusion (Figure 3C, arrows). This effect was further investigated by ROI analysis comparing the percent increase in activity from scan 2 to scan 3 for both genotypes in the ipsilateral or contralateral, dorsal and ventral hippocampus. As shown in Figure 3D, all hippocampal subregions for both genotypes showed significant percent increase in seizure induced ^{18}FDG uptake between scans 2 and 3 (*, $p < 0.05$, **$p<0.01$, ***$p<0.001$, two-tailed *t*-test). However, since the threshold for SPM analysis was set at 0.001, it became clear why the dorsal hippocampus of CD11b-HSVTK+/− mice was absent in the SPM T-map (that is, its significance fell below the stringent cut off threshold). ANOVAs for both genotypes did not reveal significant differences between percent increase in hippocampal subregions (one-way ANOVA; −/−, p=0.48; +/−, p=0.36) or between genotypes (two-way ANOVA; p=0.69). Therefore, this subtle change in the ipsilateral dorsal hippocampus should be interpreted with caution, but could represent a small proportion of ^{18}FDG uptake to which healthy activated microglia contributed to. Overall, these data revealed that pilocarpine induced changes in metabolic activity which reflected regional circuits involved in mediating seizure symptoms.

The surviving CD11b-HSVTK−/− mice (n=5) were given a final scan (Scan 4: Silent period) one week after seizure induction to determine if there were any metabolic changes associated with low level (stage 1–3) seizures during the silent period (Supplemental Figure 2). Surprisingly, despite the low stage seizures, these mice did show small metabolic differences between scans 2 and 4 (panel A shows ROI data and *t*-tests; panel B shows SPM analysis with the *p* value set at 0.05, uncorrected). Using either ROI or SPM analysis, bilateral increases in ^{18}FDG uptake were apparent in the thalamus, superior colliculus (δ, ROI: p=0.08), and cerebellum. Bilateral decreases were observed in the anterior striatum (δ, ROI: p=0.09), cortical amygdaloid nucleus, piriform cortex and dorsolateral entorhinal cortex (*, combined ROI: p=0.04). Unilateral decreases were observed in the ipsilateral somatosensory cortex. Two days following scan 4, the mice were transcardially perfused with 4% PFA and examined histologically. Microglial activation was apparent especially in the CA1, CA3 and the DG hippocampal subregions (Supplemental Figure 2C). Hippocampal neuronal survival was visualized by cresyl violet and revealed absence of neuronal death in these mice.

Activated microglia and LPS preconditioning modulate seizure threshold through the mossy fiber pathway

Our final experiment was aimed at evaluating the cellular effects of activated microglia and LPS preconditioning following SE to begin to understand the mechanism of divergent acute seizure symptoms. Since the mortality rate for group V (GCV+LPS+PILO) was 86%, we repeated the seizure induction experiments but lowered the dose of pilocarpine used (260 mg/kg for group VI) in an effort to extend the experimental time-course. The brain tissue was collected 3 days following SE induction (Figure 4A). The overall scores for each genotype were 1.24±0.07 (CD11b-HSVTK−/−, n=10) and 2.68±0.30 (CD11b-HSVTK+/−, n=13), (p=0.0005 *t*-test, Figure 4B). At this lower pilocarpine dose, mortality from acute seizures was also lower [0/10 (0%) and 2/13 (15%) in −/− and +/− mice respectively]. Seizure symptoms over the 60-minute observation period were again more severe in CD11b-HSVTK+/− mice compared to CD11b-HSVTK−/− (Figure 4C, $p<0.0001$, two-way ANOVA with Bonferroni post-tests, *$p<0.05$, **$p<0.01$, ***$p<0.001$).

CD11b-HSVTK−/− mice fully recovered showing no further symptoms, whereas 45% (5/11) of CD11b-HSVTK+/− mice displayed immobility, stiffness, arched back, lack of grooming, and weight loss over the subsequent 3 days, potentially suggesting that they never fully

recovered from SE. Moreover, when these mice were touched or lifted, a spontaneous seizure would occur reaching stages 3–5. While this was an unexpected and not quantified result, this behavior was none the less noted.

The state of microglial activation was evaluated using immunofluorescence. Robust microglial activation (Iba1+ cells) was evident in the CA1 and DG regions of the CD11b-HSVTK−/− mice on day 3, while significantly less cell counts were observed in CD11b-HSVTK+/− animals, confirming that GCV was successful in eliminating the cells (quantification given in Figure 4D, and representative staining shown in Figure 4E). Astrocytic activation was assessed using GFAP immunohistochemistry, but no differences were observed between groups for either number of reactive cells or morphology (data not shown), and has also been shown by (Falsig et al., 2008). Coincident with observed behavioral seizure symptoms, CD11b-HSVTK +/− animals showed changes in proteolytic activity along the mossy fiber pathway. Increased tPA activity (Figure 4F, arrows in CA3 and DG designate areas of proteolytic clearing of overlay substrate), and enhanced NPY expression (Figure 4G, arrows pointing to a band of fluorescence in CD11b-HSVTK+/− adjacent to the CA3 pyramidal layer) was observed in CD11b-HSVTK+/− mice that had experienced SE. tPA activity was measured as mean area of clearing over total hippocampus ± s.e.m. (CD11b-HSVTK−/−, CA3 3.6 ± 0.51, DG 0.88 ± 0.63, n=2; CD11b-HSVTK+/−, CA3 4.2 ± 0.55, DG 3.0 ± 0.27, n=2). NPY immunoreactivity in the CA3 was not detectable in CD11b-HSVTK−/− mice (0/3) but was observed in CD11b-HSVTK+/− mice coincident with SE (2/4).

We have previously shown that extracellular tPA plays a role of facilitator in mossy fiber sprouting (Carroll et al., 1994; Tsirka et al., 1995; Wu et al., 2000; Zhang et al., 2005). Several investigators have demonstrated NPY expression as an endogenous mechanism of ‘coping’ with aberrant neuronal rewiring following SE in animal models and humans (Sperk et al., 2007; Thom et al., 2009). The results presented support this notion and suggest an adaptive response to the increased hippocampal neuronal activity associated with pilocarpine induced SE in the transgenic mice. Specifically, increased tPA and NPY expression suggest that the differences in acute seizure behavior between genotypes may involve the mossy fiber pathway. Future experiments could examine additional time points in the latent period, and also during SRS.

Discussion

Striking differences in acute seizure symptoms were observed between Cd11b-HSVTK−/− and Cd11b-HSVTK+/− mice when LPS preconditioning was combined with unilateral hippocampal microglia ablation. The seizure score differences were consistent at two doses of pilocarpine (260 mg/kg and 280 mg/kg). In this experimental paradigm, the only quantifiable cellular difference between Cd11b-HSVTK−/− and Cd11b-HSVTK+/− mice (in groups V and VI) was the numbers of activated microglia/macrophages in the hippocampus. A significant reduction in the number of activated hippocampal microglia/macrophages was observed, suggesting that the activation state of microglia in the hippocampus can have a direct impact on sensitivity to acutely induced seizures. The higher seizure scores in mice lacking microglia would suggest that preconditioned microglia/macrophages may function in a protective way. This could become particularly important in maintaining a balance of hippocampal function during seizure generation and/or propagation.

We hypothesized that microglia ablation could alter the balance of inflammatory mediators in the brain, and potentially neuronal functioning as well which might change the threshold to pilocarpine induced seizures. Surprisingly however, we did not find any differences in seizure susceptibility when quiescent microglia were ablated. Instead, we found that ablation of activated microglia (by LPS preconditioning) significantly impacted seizure threshold. It

would be important to go back and measure cytokines and other inflammatory markers (proteases, reactive oxygen species) in the hippocampus following microglia ablation by GCV infusion (before and after LPS) in order to examine alternative reasons for this effect, namely potentially ongoing brain inflammation due to the killing of microglia cells. Despite this caveat, our results are consistent with the interpretation that absence of activated hippocampal microglia significantly reduced seizure threshold.

Although the relationship between microglial activation and neurodegenerative disease is not completely understood, there is a great deal of evidence supporting a pathological role for microglia in the progression of disease (Beach et al., 1995; Taniwaki et al., 1996; van Vliet et al., 2007). Severe acute seizures caused by pilocarpine are known to progress into a silent period (lasting from a few days post SE, to about a month), where neuronal death, gliosis and rewiring of circuitry presumably occur. This is followed by a chronic phase where spontaneous recurrent seizures (SRS) can take place (Borges et al., 2003; Shibley and Smith, 2002). During severe SRS activated microglia are observed in the same hippocampal regions associated with neuronal death (Borges et al., 2003; Taniwaki et al., 1996; Tooyama et al., 2002) suggesting that they function as neurotoxic mediators, but recent studies have suggested that their impact can be far more complex.

The primary function of activated microglia in the brain is thought to be the return of injured tissue to homeostasis (Streit and Xue, 2009). Excitotoxic insult causes quiescent ramified microglia to become activated, morphologically become amoeboid, and phagocytose dead cells. Potentially neurotoxic substances are concurrently secreted including nitric oxide (NO), reactive oxygen species (ROS), cycloxygenases, proteases, and proinflammatory cytokines, which can further damage the neurons. This secondary death is decreased when microglial activation is inhibited (Rogove and Tsirka, 1998; Wang et al., 2003), and as shown here via microglia ablation (suppl fig 1). Interleukin-1β (IL-1β), for example, is upregulated during kindling (Plata-Salaman et al., 2000) and has been targeted as a contributory factor in epilepsy (Ravizza et al., 2006).

Studies also suggest, however, that activated microglia can release neurotrophins and other positive factors to promote neuronal stability (Elkabes et al., 1996). This effect is particularly interesting in the context of preconditioning, where several studies have shown that LPS-stimulated rat brain microglia/macrophages can release nerve growth factor (NGF) and brain-derived neurotropic factor (BDNF) (Elkabes et al., 1998; Heese et al., 1998; Miwa et al., 1997; Nakajima et al., 2001a; Xiong et al., 1999), molecules known to promote neuronal recovery from injury. Preconditioning with LPS (allowing time for recovery from the acute LPS-induced inflammation) may facilitate an accumulation of protective factors, or initiate a compensatory or adaptive response to excitotoxic insult. This effect may be similar to the neuroprotection observed following preconditioning with brief kainate-induced seizures prior to prolonged SE, which resulted in upregulation of both neuronal genes associated with structural changes and signaling, and glial genes such as upregulated glutamate transporters (Borges et al., 2007). The timing of this pre-activation in relation to the insult seems to be crucial in the net effect of the glial response. This is evident in PTZ-induced seizures, where LPS given early (1–4 hours) was pro-convulsant, but later administration (18–24 hours) had anticonvulsant effects, (Akarsu et al., 2006; Sayyah et al., 2003a). Furthermore, a recent study showed LPS preconditioning could actually protect hippocampal neurons from a typical neurodegenerative fate, although in this study the dose used (0.5 mg/kg) did not affect seizure symptoms (Dmowska et al., 2009).

LPS-induced neuroinflammation has also been shown to decrease and modulate hippocampal neurogenesis (Ekdahl et al., 2003; Monje et al., 2003; Yang et al., 2009). In a recent study, LPS injected into the DG of the hippocampus resulted in enhanced inhibitory synaptic drive

of adult-born integrated neurons, which was thought to be a compensatory response to the inflammation (Jakubs et al., 2008). However, several studies have also shown that reactive gliosis (microglia and astrocytes) can lead to damage or permanent hyperexcitability of neurons (Binder and Steinhauser, 2006) by promoting synaptogenesis and synaptic remodeling (Cullheim and Thams, 2007; Wake et al., 2009). SE can induce aberrant hippocampal neurogenesis, which often leads to a recurrent excitatory circuitry. Whether preconditioning-mediated LPS-induced plasticity could modulate adaptive responses to excessive neuronal firing during seizures remains to be explored.

Recycling of extracellular glutamate is normally an astrocyte specific responsibility, but activated microglia expressing the high-affinity glutamate transporter GLT-1 can contribute approximately 10% to it (Persson et al., 2005; Shaked et al., 2005). 12 hours after LPS administration the capability of microglia to take up glutamate has been reported to be significantly increased through enhanced expression of GLT-1 (Jacobsson et al., 2006; Persson et al., 2005), which in our study, could be a major contributing factor to the increased seizure sensitivity seen after microglia/macrophage ablation. Additionally, microglial/macrophage glutamate uptake has been shown to reduce glutamate-induced neuronal death *in vitro* (Rimaniol et al., 2000). The glutamate uptake is then coupled with a concomitant increase in glutathione synthesis, which could provide another protective mechanism via enhanced antioxidant capacity (Persson et al., 2006). Recent evidence, showing that astrocytes in the hilar region are highly susceptible to damage caused by seizures (Borges et al., 2006; Kang et al., 2006), supports the notion that microglial glutamate uptake may be a back-up system for astrocytes during pathological conditions (Nakajima et al., 2001b; Persson et al., 2005; Rimaniol et al., 2000). Therefore, in our study, ablation of preconditioned microglia could be severely detrimental during acute seizures, as glutamate clearance from the extracellular milieu would be affected. These data have physiological relevance as patients with TLE were shown to have reduced glutamate/glutamine cycles and altered expression of important components of the cycle, such as the glial glutamate transporters (Petroff et al., 2002).

Small animal imaging has increasingly become an important tool used to understand changes in the brain due to acute and chronic seizures in animal models (Dedeurwaerdere et al., 2007; Jupp and O'Brien, 2007; Jupp et al., 2006; Liefaard et al., 2009; Navarro Mora et al., 2009; O'Brien and Jupp, 2009; Yakushev et al., 2009). The advantage of using imaging approaches to study seizure disorders is that animals can be evaluated at several time points spanning seizure induction, the latent period, and development of SRS, in addition to response to various therapies. Also, these measures are on a systems level (albeit with limited resolution), but can provide novel clues for regional network activity changes that may correlate with different stages of the disease. Studies have shown that early on in the silent period there is decreased metabolism in the hippocampus, thalamus, and entorhinal cortex (Goffin et al., 2009; Guo et al., 2009), which are regions of increased metabolism during the seizures (Kornblum et al., 2000; Mirrione et al., 2007; Mirrione et al., 2006). This decreased metabolism could represent recovery from excessive neuronal firing and/or a progression of neuronal changes which lead to SRS. Our study suggests that activated microglia/macrophages may provide some component of the metabolic signature during acute seizures (either directly, or indirectly through modulating neuronal activation), as their ablation correlates with less hippocampal ^{18}FDG uptake compared to the contralateral side. This interpretation is supported by literature suggesting astrocytes contribute to the metabolic signal (Magistretti and Pellerin, 1996; Magistretti and Pellerin, 2000), and one recent PET study showing microglia activation corresponds to increased metabolic demand in the peri-infarct zone of a rat model of ischemia (Schroeter et al., 2009).

Interestingly, it has been suggested that kainate preconditioning may render vulnerable hippocampal neurons more resistant to prolonged ATP-depleting damage, as such caused by

seizures (Borges et al., 2007), and this process could be compromised by microglia/macrophage ablation. Our results are consistent with well established histological studies showing progressive damage in affected areas including the endopiriform nucleus, piriform cortex entorhrinal cortex, amygdaloid nuclei, and thalamus (Leite et al., 1990; Turski et al., 1984; Turski et al., 1983a). Further studies combining in-vivo imaging techniques with postmortem high resolution end-point methods, such as microscopy, will contribute a more integrated understanding of pathology associated with metabolic changes during epileptogenesis (O'Brien and Jupp, 2009).

These data demonstrate the usefulness of imaging the same animals over time to evaluate metabolic changes corresponding to the different stages that follow pilocarpine induced SE. Interestingly, we observed apparent changes in ^{18}FDG uptake despite lack of generalized seizures. This result may be consistent with a recent study reporting that pilocarpine-injected rats developed spontaneous recurrent seizures (SRS), even in the absence of initial SE, after a long latency period (Navarro Mora et al., 2009). In a separate report, the availability of the dopamine $D_{2/3}$ receptor in the anterior striatum was 27% lower in pilocarpine-treated rats during the chronic phase (Yakushev et al., 2009), which could correlate with the changes we observed in that region. It is also noteworthy that despite the lack of generalized seizures, the regions visualized corresponded to typical locations of neuronal damage, such as the septum, thalamus, amygaloid complex, piriform and entorhinal cortices (Turski et al., 1983b).

A decrease or absence of the typical latent period in these mice suggests that microglia may be involved not only in acute seizure symptoms, but also in epileptogenesis itself (the process whereby spontaneous recurrent seizures develop following abnormal plasticity). The microglia may contribute to plasticity through diffusible factors which can modulate synaptic strength [for example studies have shown that TNF-alpha increases surface expression of AMPA receptors in the synapse (Beattie et al., 2002; Savin et al., 2009; Stellwagen and Malenka, 2006)], can regulate potassium and calcium (Beck et al., 2008; Kofuji and Newman, 2004), and secrete neurotrophins which may aid injured neurons in recovery from the initial epileptic event (Miwa et al., 1997; Nakajima et al., 2001a). In the case of the mice used in this study, upon ablation of functional microglia, which would normally phagocytose necrotic neurons (and other necrotic or apoptotic neighboring cells and cell debris), plasticity of surviving neurons and glia could indeed be altered, and manifest itself as early handling-induced seizures or lack of recovery from acute seizures.

Taken together, our data show that seizure symptoms were decreased for CD11b-HSVTK−/− and increased for CD11b-HSVTK+/− mice following LPS preconditioning and microglia/macrophage ablation. LPS pretreatment affected the number of mice experiencing higher stage seizures at both doses of pilocarpine used in this study.

Although our data focus only on the pilocarpine model of seizures (along with kainate neurotoxicity), other models could be investigated including kainate induced epileptogenesis and kindling. It would be interesting to evaluate whether similar pro-convulsant properties are exhibited when preconditioned microglia are ablated in these models. If similar trends are observed with kainate induced seizures, such result might directly suggest that glutamate release can be modulated by microglia to influence neuronal firing. In fact, evidence suggests that in kainate induced seizures, TNF-α may actually be neuroprotective (Balosso et al., 2005; Lu et al., 2008) and IL-1β is proconvulsant by enhancing glutamate (Vezzani et al., 1999; Vezzani et al., 2000). Future studies will also address behavioral outcomes from bilateral infusions of gancyclovir in order to incorporate activity from both sides of the hippocampus. Additionally, intracerebroventricular infusion will allow us to reach not only the hippocampi, but other areas of the ventral forebrain that may also be implicated in seizure initiation.

Overall, the data presented here point towards a neuroprotective function for preconditioned hippocampal microglia/macrophages during the acute phase of seizures through potential secretion/release of factors that may be anti-convulsant. Our data support emerging literature reports investigating the interaction between the immune system and neuronal firing during seizures. It has been suggested that immunomodulatory therapies could be used to prevent trauma-induced spontaneous recurrent seizures (Rodgers et al., 2009), and treat other forms of epilepsy (Billiau et al., 2005). While this is an intriguing possibility, a continued critical evaluation of the timing of microglia activation and releasable factors that influence neurons during epileptogeneis is warranted.

Supplementary Material

Refer to Web version on PubMed Central for supplementary material.

Acknowledgments

This work was supported by National Institutes of Health, RO1NS42168 and American Heart Association-Established Investigator Award (to S.E.T.), R01NS046006 to F.L.H., National Institute on Drug Abuse (DA15041) and the Department of Energy (to S.L.D), and National Science Foundation Integrative Graduate Education and Research Traineeship, Minerals, Metals, Metalloids, and Toxicity (to S.E.T. and M.M.M). Grants to FLH by the DFG (SFB TRR43 and Exc 25). The authors would like to thank Drs. Joanna Fowler, Marian Evinger, and Joav Prives for helpful suggestions, and Dr. Holly Colognato for sharing equipment. Also, we would like to thank members of the BNL cyclotron facility, Dave Alexoff, Michael Schueller, David J. Schyler, Colleen Shea, and Youwen Xu for ^{18}FDG preparation.

References

Akarsu ES, Ozdayi S, Algan E, Ulupinar F. The neuronal excitability time-dependently changes after lipopolysaccharide administration in mice: possible role of cyclooxygenase-2 induction. Epilepsy Res 2006;71:181–7. [PubMed: 16870400]

Altay EE, Fessler AJ, Gallagher M, Attarian HP, Dehdashti F, Vahle VJ, Ojemann J, Dowling JL, Gilliam FG. Correlation of severity of FDG-PET hypometabolism and interictal regional delta slowing in temporal lobe epilepsy. Epilepsia 2005;46:573–6. [PubMed: 15816953]

Arican N, Kaya M, Kalayci R, Uzun H, Ahishali B, Bilgic B, Elmas I, Kucuk M, Gurses C, Uzun M. Effects of lipopolysaccharide on blood-brain barrier permeability during pentylenetetrazole-induced epileptic seizures in rats. Life Sci 2006;79:1–7. [PubMed: 16434059]

Auvin S, Porta N, Nehlig A, Lecointe C, Vallee L, Bordet R. Inflammation in rat pups subjected to short hyperthermic seizures enhances brain long-term excitability. Epilepsy Res 2009;86:124–30. [PubMed: 19535227]

Balosso S, Ravizza T, Perego C, Peschon J, Campbell IL, De Simoni MG, Vezzani A. Tumor necrosis factor-alpha inhibits seizures in mice via p75 receptors. Ann Neurol 2005;57:804–12. [PubMed: 15852477]

Beach TG, Woodhurst WB, MacDonald DB, Jones MW. Reactive microglia in hippocampal sclerosis associated with human temporal lobe epilepsy. Neurosci Lett 1995;191:27–30. [PubMed: 7659283]

Beattie EC, Stellwagen D, Morishita W, Bresnahan JC, Ha BK, Von Zastrow M, Beattie MS, Malenka RC. Control of synaptic strength by glial TNFalpha. Science 2002;295:2282–5. [PubMed: 11910117]

Beck A, Penner R, Fleig A. Lipopolysaccharide-induced down-regulation of Ca2+ release-activated Ca2+ currents (I CRAC) but not Ca2+-activated TRPM4-like currents (I CAN) in cultured mouse microglial cells. J Physiol 2008;586:427–39. [PubMed: 17991695]

Billiau AD, Wouters CH, Lagae LG. Epilepsy and the immune system: is there a link? Eur J Paediatr Neurol 2005;9:29–42. [PubMed: 15701565]

Binder DK, Steinhauser C. Functional changes in astroglial cells in epilepsy. Glia 2006;54:358–68. [PubMed: 16886201]

Borges K, Gearing M, McDermott DL, Smith AB, Almonte AG, Wainer BH, Dingledine R. Neuronal and glial pathological changes during epileptogenesis in the mouse pilocarpine model. Experimental Neurology 2003;182:21–34. [PubMed: 12821374]

Borges K, McDermott D, Irier H, Smith Y, Dingledine R. Degeneration and proliferation of astrocytes in the mouse dentate gyrus after pilocarpine-induced status epilepticus. Exp Neurol 2006;201:416–27. [PubMed: 16793040]

Borges K, Shaw R, Dingledine R. Gene expression changes after seizure preconditioning in the three major hippocampal cell layers. Neurobiol Dis 2007;26:66–77. [PubMed: 17239605]

Carroll PM, Tsirka SE, Richards WG, Frohman MA, Strickland S. The mouse tissue plasminogen activator gene 5′ flanking region directs appropriate expression in development and a seizure-enhanced response in the CNS. Development 1994;120:3173–83. [PubMed: 7720560]

Coulter DA. Epilepsy-associated plasticity in gamma-aminobutyric acid receptor expression, function, and inhibitory synaptic properties. International Review of Neurobiology 2001;45:237–52. [PubMed: 11130901]

Cullheim S, Thams S. The microglial networks of the brain and their role in neuronal network plasticity after lesion. Brain Res Rev 2007;55:89–96. [PubMed: 17509690]

de Bock F, Dornand J, Rondouin G. Release of TNF alpha in the rat hippocampus following epileptic seizures and excitotoxic neuronal damage. Neuroreport 1996;7:1125–9. [PubMed: 8817515]

Dedeurwaerdere S, Jupp B, O'Brien TJ. Positron Emission Tomography in basic epilepsy research: a view of the epileptic brain. Epilepsia 2007;48(Suppl 4):56–64. [PubMed: 17767576]

Dmowska M, Cybulska R, Schoenborn R, Piersiak T, Jaworska-Adamu J, Gawron A. Behavioural and Histological Effects of Preconditioning with Lipopolysaccharide in Epileptic Rats. Neurochem Res. 2009

Drage MG, Holmes GL, Seyfried TN. Hippocampal neurons and glia in epileptic EL mice. J Neurocytol 2002;31:681–92. [PubMed: 14501207]

Ekdahl CT, Claasen JH, Bonde S, Kokaia Z, Lindvall O. Inflammation is detrimental for neurogenesis in adult brain. Proc Natl Acad Sci U S A 2003;100:13632–7. [PubMed: 14581618]

Elkabes S, DiCicco-Bloom EM, Black IB. Brain microglia/macrophages express neurotrophins that selectively regulate microglial proliferation and function. J Neurosci 1996;16:2508–21. [PubMed: 8786427]

Elkabes S, Peng L, Black IB. Lipopolysaccharide differentially regulates microglial trk receptor and neurotrophin expression. J Neurosci Res 1998;54:117–22. [PubMed: 9778155]

Falsig J, Julius C, Margalith I, Schwarz P, Heppner FL, Aguzzi A. A versatile prion replication assay in organotypic brain slices. Nat Neurosci 2008;11:109–17. [PubMed: 18066056]

Goffin K, Van Paesschen W, Dupont P, Van Laere K. Longitudinal microPET imaging of brain glucose metabolism in rat lithium-pilocarpine model of epilepsy. Exp Neurol 2009;217:205–9. [PubMed: 19236862]

Gravanis I, Tsirka SE. Tissue plasminogen activator and glial function. Glia. 2004

Guo Y, Gao F, Wang S, Ding Y, Zhang H, Wang J, Ding MP. In vivo mapping of temporospatial changes in glucose utilization in rat brain during epileptogenesis: an 18F-fluorodeoxyglucose-small animal positron emission tomography study. Neuroscience 2009;162:972–9. [PubMed: 19477240]

Heese K, Fiebich BL, Bauer J, Otten U. NF-kappaB modulates lipopolysaccharide-induced microglial nerve growth factor expression. Glia 1998;22:401–7. [PubMed: 9517572]

Heppner FL, Greter M, Marino D, Falsig J, Raivich G, Hovelmeyer N, Waisman A, Rulicke T, Prinz M, Priller J, Becher B, Aguzzi A. Experimental autoimmune encephalomyelitis repressed by microglial paralysis. Nat Med 2005;11:146–52. [PubMed: 15665833]

Jacobsson J, Persson M, Hansson E, Ronnback L. Corticosterone inhibits expression of the microglial glutamate transporter GLT-1 in vitro. Neuroscience 2006;139:475–83. [PubMed: 16473474]

Jakubs K, Bonde S, Iosif RE, Ekdahl CT, Kokaia Z, Kokaia M, Lindvall O. Inflammation regulates functional integration of neurons born in adult brain. J Neurosci 2008;28:12477–88. [PubMed: 19020040]

Jupp B, O'Brien TJ. Application of coregistration for imaging of animal models of epilepsy. Epilepsia 2007;48(Suppl 4):82–9. [PubMed: 17767579]

Jupp B, Williams JP, Tesiram YA, Vosmansky M, O'Brien TJ. Hippocampal T2 signal change during amygdala kindling epileptogenesis. Epilepsia 2006;47:41–6. [PubMed: 16417530]

Kang TC, Kim DS, Kwak SE, Kim JE, Won MH, Kim DW, Choi SY, Kwon OS. Epileptogenic roles of astroglial death and regeneration in the dentate gyrus of experimental temporal lobe epilepsy. Glia 2006;54:258–71. [PubMed: 16845674]

Kofuji P, Newman EA. Potassium buffering in the central nervous system. Neuroscience 2004;129:1045–56. [PubMed: 15561419]

Kornblum HI, Araujo DM, Annala AJ, Tatsukawa KJ, Phelps ME, Cherry SR. In vivo imaging of neuronal activation and plasticity in the rat brain by high resolution positron emission tomography (microPET). Nat Biotechnol 2000;18:655–60. [PubMed: 10835605]

Lamusuo S, Jutila L, Ylinen A, Kalviainen R, Mervaala E, Haaparanta M, Jaaskelainen S, Partanen K, Vapalahti M, Rinne J. [18F]FDG-PET reveals temporal hypometabolism in patients with temporal lobe epilepsy even when quantitative MRI and histopathological analysis show only mild hippocampal damage. Arch Neurol 2001;58:933–9. [PubMed: 11405808]

Leite JP, Bortolotto ZA, Cavalheiro EA. Spontaneous recurrent seizures in rats: an experimental model of partial epilepsy. Neurosci Biobehav Rev 1990;14:511–7. [PubMed: 2287490]

Liefaard LC, Ploeger BA, Molthoff CF, de Jong HW, Dijkstra J, van der Weerd L, Lammertsma AA, Danhof M, Voskuyl RA. Changes in GABAA receptor properties in amygdala kindled animals: in vivo studies using [11C]flumazenil and positron emission tomography. Epilepsia 2009;50:88–98. [PubMed: 18727682]

Lu MO, Zhang XM, Mix E, Quezada HC, Jin T, Zhu J, Adem A. TNF-alpha receptor 1 deficiency enhances kainic acid-induced hippocampal injury in mice. J Neurosci Res 2008;86:1608–14. [PubMed: 18189316]

Ma Y, Hof PR, Grant SC, Blackband SJ, Bennett R, Slatest L, McGuigan MD, Benveniste H. A three-dimensional digital atlas database of the adult C57BL/6J mouse brain by magnetic resonance microscopy. Neuroscience 2005;135:1203–15. [PubMed: 16165303]

Magistretti PJ, Pellerin L. The contribution of astrocytes to the 18F-2-deoxyglucose signal in PET activation studies. Mol Psychiatry 1996;1:445–52. [PubMed: 9154245]

Magistretti PJ, Pellerin L. [Functional brain imaging: role metabolic coupling between astrocytes and neurons]. Rev Med Suisse Romande 2000;120:739–42. [PubMed: 11094539]

Marsh B, Stevens SL, Packard AE, Gopalan B, Hunter B, Leung PY, Harrington CA, Stenzel-Poore MP. Systemic lipopolysaccharide protects the brain from ischemic injury by reprogramming the response of the brain to stroke: a critical role for IRF3. J Neurosci 2009a;29:9839–49. [PubMed: 19657036]

Marsh BJ, Williams-Karnesky RL, Stenzel-Poore MP. Toll-like receptor signaling in endogenous neuroprotection and stroke. Neuroscience 2009b;158:1007–20. [PubMed: 18809468]

Mirrione MM, Schiffer WK, Fowler JS, Alexoff DL, Dewey SL, Tsirka SE. A novel approach for imaging brain-behavior relationships in mice reveals unexpected metabolic patterns during seizures in the absence of tissue plasminogen activator. Neuroimage 2007;38:34–42. [PubMed: 17707126]

Mirrione MM, Schiffer WK, Siddiq M, Dewey SL, Tsirka SE. PET imaging of glucose metabolism in a mouse model of temporal lobe epilepsy. Synapse 2006;59:119–21. [PubMed: 16320304]

Miwa T, Furukawa S, Nakajima K, Furukawa Y, Kohsaka S. Lipopolysaccharide enhances synthesis of brain-derived neurotrophic factor in cultured rat microglia. J Neurosci Res 1997;50:1023–9. [PubMed: 9452017]

Monje ML, Toda H, Palmer TD. Inflammatory blockade restores adult hippocampal neurogenesis. Science 2003;302:1760–5. [PubMed: 14615545]

Nakajima K, Honda S, Tohyama Y, Imai Y, Kohsaka S, Kurihara T. Neurotrophin secretion from cultured microglia. J Neurosci Res 2001a;65:322–31. [PubMed: 11494368]

Nakajima K, Tohyama Y, Kohsaka S, Kurihara T. Ability of rat microglia to uptake extracellular glutamate. Neurosci Lett 2001b;307:171–4. [PubMed: 11438391]

Navarro Mora G, Bramanti P, Osculati F, Chakir A, Nicolato E, Marzola P, Sbarbati A, Fabene PF. Does pilocarpine-induced epilepsy in adult rats require status epilepticus? PLoS One 2009;4:e5759. [PubMed: 19503612]

O'Brien TJ, Jupp B. In-vivo imaging with small animal FDG-PET: a tool to unlock the secrets of epileptogenesis? Exp Neurol 2009;220:1–4. [PubMed: 19646437]

Persson M, Brantefjord M, Hansson E, Ronnback L. Lipopolysaccharide increases microglial GLT-1 expression and glutamate uptake capacity in vitro by a mechanism dependent on TNF-alpha. Glia 2005;51:111–20. [PubMed: 15789431]

Persson M, Sandberg M, Hansson E, Ronnback L. Microglial glutamate uptake is coupled to glutathione synthesis and glutamate release. Eur J Neurosci 2006;24:1063–70. [PubMed: 16925588]

Petroff OA, Errante LD, Rothman DL, Kim JH, Spencer DD. Glutamate-glutamine cycling in the epileptic human hippocampus. Epilepsia 2002;43:703–10. [PubMed: 12102672]

Pierce JP, Melton J, Punsoni M, McCloskey DP, Scharfman HE. Mossy fibers are the primary source of afferent input to ectopic granule cells that are born after pilocarpine-induced seizures. Exp Neurol 2005;196:316–31. [PubMed: 16342370]

Plata-Salaman CR, Ilyin SE, Turrin NP, Gayle D, Flynn MC, Romanovitch AE, Kelly ME, Bureau Y, Anisman H, McIntyre DC. Kindling modulates the IL-1beta system, TNF-alpha, TGF-beta1, and neuropeptide mRNAs in specific brain regions. Brain Res Mol Brain Res 2000;75:248–58. [PubMed: 10686345]

Racine RJ, Gartner JG, Burnham WM. Epileptiform activity and neural plasticity in limbic structures. Brain Res 1972;47:262–8. [PubMed: 4641271]

Ravizza T, Gagliardi B, Noe F, Boer K, Aronica E, Vezzani A. Innate and adaptive immunity during epileptogenesis and spontaneous seizures: evidence from experimental models and human temporal lobe epilepsy. Neurobiol Dis 2008;29:142–60. [PubMed: 17931873]

Ravizza T, Lucas SM, Balosso S, Bernardino L, Ku G, Noe F, Malva J, Randle JC, Allan S, Vezzani A. Inactivation of caspase-1 in rodent brain: a novel anticonvulsive strategy. Epilepsia 2006;47:1160–8. [PubMed: 16886979]

Riazi K, Galic MA, Kuzmiski JB, Ho W, Sharkey KA, Pittman QJ. Microglial activation and TNFalpha production mediate altered CNS excitability following peripheral inflammation. Proc Natl Acad Sci U S A 2008;105:17151–6. [PubMed: 18955701]

Rimaniol AC, Haik S, Martin M, Le Grand R, Boussin FD, Dereuddre-Bosquet N, Gras G, Dormont D. Na+-dependent high-affinity glutamate transport in macrophages. J Immunol 2000;164:5430–8. [PubMed: 10799909]

Rodgers KM, Hutchinson MR, Northcutt A, Maier SF, Watkins LR, Barth DS. The cortical innate immune response increases local neuronal excitability leading to seizures. Brain 2009;132:2478–86. [PubMed: 19567702]

Rogove AD, Siao C, Keyt B, Strickland S, Tsirka SE. Activation of microglia reveals a non-proteolytic cytokine function for tissue plasminogen activator in the central nervous system. J Cell Sci 1999;112 (Pt 22):4007–16. [PubMed: 10547361]

Rogove AD, Tsirka SE. Neurotoxic responses by microglia elicited by excitotoxic injury in the mouse hippocampus. Curr Biol 1998;8:19–25. [PubMed: 9427623]

Rosenzweig HL, Lessov NS, Henshall DC, Minami M, Simon RP, Stenzel-Poore MP. Endotoxin preconditioning prevents cellular inflammatory response during ischemic neuroprotection in mice. Stroke 2004;35:2576–81. [PubMed: 15375302]

Saha RN, Ghosh A, Palencia CA, Fung YK, Dudek SM, Pahan K. TNF-alpha preconditioning protects neurons via neuron-specific up-regulation of CREB-binding protein. J Immunol 2009;183:2068–78. [PubMed: 19596989]

Sankar R, Auvin S, Mazarati A, Shin D. Inflammation contributes to seizure-induced hippocampal injury in the neonatal rat brain. Acta Neurol Scand 2007;115:16–20. [PubMed: 17362271]

Savin C, Triesch J, Meyer-Hermann M. Epileptogenesis due to glia-mediated synaptic scaling. J R Soc Interface 2009;6:655–68. [PubMed: 18986963]

Sayyah M, Javad-Pour M, Ghazi-Khansari M. The bacterial endotoxin lipopolysaccharide enhances seizure susceptibility in mice: involvement of proinflammatory factors: nitric oxide and prostaglandins. Neuroscience 2003a;122:1073–80. [PubMed: 14643773]

Sayyah M, Najafabadi IT, Beheshti S, Majzoob S. Lipopolysaccharide retards development of amygdala kindling but does not affect fully-kindled seizures in rats. Epilepsy Res 2003b;57:175–80. [PubMed: 15013059]

Schauwecker PE, Steward O. Genetic determinants of susceptibility to excitotoxic cell death: Implications for gene targeting approaches. PNAS 1997;94:4103–4108. [PubMed: 9108112]

Schiffer WK, Mirrione MM, Biegon A, Alexoff DL, Patel V, Dewey SL. Serial microPET measures of the metabolic reaction to a microdialysis probe implant. J Neurosci Methods. 2006

Schroeter M, Dennin MA, Walberer M, Backes H, Neumaier B, Fink GR, Graf R. Neuroinflammation extends brain tissue at risk to vital peri-infarct tissue: a double tracer [11C]PK11195- and [18F]FDG-PET study. J Cereb Blood Flow Metab 2009;29:1216–25. [PubMed: 19352400]

Schwartz M, Butovsky O, Bruck W, Hanisch UK. Microglial phenotype: is the commitment reversible? Trends Neurosci 2006;29:68–74. [PubMed: 16406093]

Shaked I, Tchoresh D, Gersner R, Meiri G, Mordechai S, Xiao X, Hart RP, Schwartz M. Protective autoimmunity: interferon-gamma enables microglia to remove glutamate without evoking inflammatory mediators. J Neurochem 2005;92:997–1009. [PubMed: 15715651]

Shapiro LA, Wang L, Ribak CE. Rapid astrocyte and microglial activation following pilocarpine-induced seizures in rats. Epilepsia 2008;49(Suppl 2):33–41. [PubMed: 18226170]

Sheehan JJ, Zhou C, Gravanis I, Rogove AD, Wu YP, Bogenhagen DF, Tsirka SE. Proteolytic activation of monocyte chemoattractant protein-1 by plasmin underlies excitotoxic neurodegeneration in mice. J Neurosci 2007;27:1738–45. [PubMed: 17301181]

Shibley H, Smith BN. Pilocarpine-induced status epilepticus results in mossy fiber sprouting and spontaneous seizures in C57BL/6 and CD-1 mice. Epilepsy Res 2002;49:109–20. [PubMed: 12049799]

Siao CJ, Fernandez SR, Tsirka SE. Cell type-specific roles for tissue plasminogen activator released by neurons or microglia after excitotoxic injury. J Neurosci 2003;23:3234–42. [PubMed: 12716930]

Siao CJ, Tsirka SE. Tissue plasminogen activator mediates microglial activation via its finger domain through annexin II. J Neurosci 2002;22:3352–8. [PubMed: 11978811]

Sperk G, Hamilton T, Colmers WF. Neuropeptide Y in the dentate gyrus. Prog Brain Res 2007;163:285–97. [PubMed: 17765725]

Stellwagen D, Malenka RC. Synaptic scaling mediated by glial TNF-alpha. Nature 2006;440:1054–9. [PubMed: 16547515]

Streit WJ, Walter SA, Pennell NA. Reactive microgliosis. Prog Neurobiol 1999;57:563–81. [PubMed: 10221782]

Streit WJ, Xue QS. Life and Death of Microglia. J Neuroimmune Pharmacol. 2009

Taniwaki Y, Kato M, Araki T, Kobayashi T. Microglial activation by epileptic activities through the propagation pathway of kainic acid-induced hippocampal seizures in the rat. Neurosci Lett 1996;217:29–32. [PubMed: 8905732]

Thom M, Martinian L, Catarino C, Yogarajah M, Koepp MJ, Caboclo L, Sisodiya SM. Bilateral reorganization of the dentate gyrus in hippocampal sclerosis: a postmortem study. Neurology 2009;73:1033–40. [PubMed: 19710404]

Tooyama I, Bellier JP, Park M, Minnasch P, Uemura S, Hisano T, Iwami M, Aimi Y, Yasuhara O, Kimura H. Morphologic study of neuronal death, glial activation, and progenitor cell division in the hippocampus of rat models of epilepsy. Epilepsia 2002;43(Suppl 9):39–43. [PubMed: 12383279]

Tsirka SE, Gualandris A, Amaral DG, Strickland S. Excitotoxin-induced neuronal degeneration and seizure are mediated by tissue plasminogen activator. Nature 1995;377:340–4. [PubMed: 7566088]

Turrin NP, Rivest S. Innate immune reaction in response to seizures: implications for the neuropathology associated with epilepsy. Neurobiol Dis 2004;16:321–34. [PubMed: 15193289]

Turski WA, Cavalheiro EA, Bortolotto ZA, Mello LM, Schwarz M, Turski L. Seizures produced by pilocarpine in mice: a behavioral, electroencephalographic and morphological analysis. Brain Res 1984;321:237–53. [PubMed: 6498517]

Turski WA, Cavalheiro EA, Schwarz M, Czuczwar SJ, Kleinrok Z, Turski L. Limbic seizures produced by pilocarpine in rats: behavioural, electroencephalographic and neuropathological study. Behav Brain Res 1983a;9:315–35. [PubMed: 6639740]

Turski WA, Cavalheiro EA, Turski L, Kleinrok Z. Intrahippocampal bethanechol in rats: behavioural, electroencephalographic and neuropathological correlates. Behav Brain Res 1983b;7:361–70. [PubMed: 6132610]

van Vliet EA, da Costa Araujo S, Redeker S, van Schaik R, Aronica E, Gorter JA. Blood-brain barrier leakage may lead to progression of temporal lobe epilepsy. Brain 2007;130:521–34. [PubMed: 17124188]

Vezzani A, Conti M, De Luigi A, Ravizza T, Moneta D, Marchesi F, De Simoni MG. Interleukin-1beta immunoreactivity and microglia are enhanced in the rat hippocampus by focal kainate application: functional evidence for enhancement of electrographic seizures. J Neurosci 1999;19:5054–65. [PubMed: 10366638]

Vezzani A, Moneta D, Conti M, Richichi C, Ravizza T, De Luigi A, De Simoni MG, Sperk G, Andell-Jonsson S, Lundkvist J, Iverfeldt K, Bartfai T. Powerful anticonvulsant action of IL-1 receptor antagonist on intracerebral injection and astrocytic overexpression in mice. Proc Natl Acad Sci U S A 2000;97:11534–9. [PubMed: 11016948]

Vielhaber S, Von Oertzen JH, Kudin AF, Schoenfeld A, Menzel C, Biersack HJ, Kral T, Elger CE, Kunz WS. Correlation of hippocampal glucose oxidation capacity and interictal FDG-PET in temporal lobe epilepsy. Epilepsia 2003;44:193–9. [PubMed: 12558573]

Wake H, Moorhouse AJ, Jinno S, Kohsaka S, Nabekura J. Resting microglia directly monitor the functional state of synapses in vivo and determine the fate of ischemic terminals. J Neurosci 2009;29:3974–80. [PubMed: 19339593]

Wang J, Rogove AD, Tsirka AE, Tsirka SE. Protective role of tuftsin fragment 1–3 in an animal model of intracerebral hemorrhage. Ann Neurol 2003;54:655–64. [PubMed: 14595655]

Wu YP, Siao CJ, Lu W, Sung TC, Frohman MA, Milev P, Bugge TH, Degen JL, Levine JM, Margolis RU, Tsirka SE. The tissue plasminogen activator (tPA)/plasmin extracellular proteolytic system regulates seizure-induced hippocampal mossy fiber outgrowth through a proteoglycan substrate. J Cell Biol 2000;148:1295–304. [PubMed: 10725341]

Xiong H, Yamada K, Jourdi H, Kawamura M, Takei N, Han D, Nabeshima T, Nawa H. Regulation of nerve growth factor release by nitric oxide through cyclic GMP pathway in cortical glial cells. Mol Pharmacol 1999;56:339–47. [PubMed: 10419553]

Yakushev IY, Dupont E, Buchholz HG, Tillmanns J, Debus F, Cumming P, Heimann A, Fellgiebel A, Luhmann HJ, Landvogt C, Werhahn KJ, Schreckenberger M, Potschka H, Bartenstein P. In vivo imaging of dopamine receptors in a model of temporal lobe epilepsy. Epilepsia. 2009

Yang F, Liu ZR, Chen J, Zhang SJ, Quan QY, Huang YG, Jiang W. Roles of astrocytes and microglia in seizure-induced aberrant neurogenesis in the hippocampus of adult rats. J Neurosci Res. 2009

Yuhas Y, Nofech-Mozes Y, Weizman A, Ashkenazi S. Enhancement of pentylenetetrazole-induced seizures by Shigella dysenteriae in LPS-resistant C3H/HeJ mice: role of the host response. Med Microbiol Immunol 2002;190:173–8. [PubMed: 12005330]

Zhang Y, Kanaho Y, Frohman MA, Tsirka SE. Phospholipase D1-promoted release of tissue plasminogen activator facilitates neurite outgrowth. J Neurosci 2005;25:1797–805. [PubMed: 15716416]

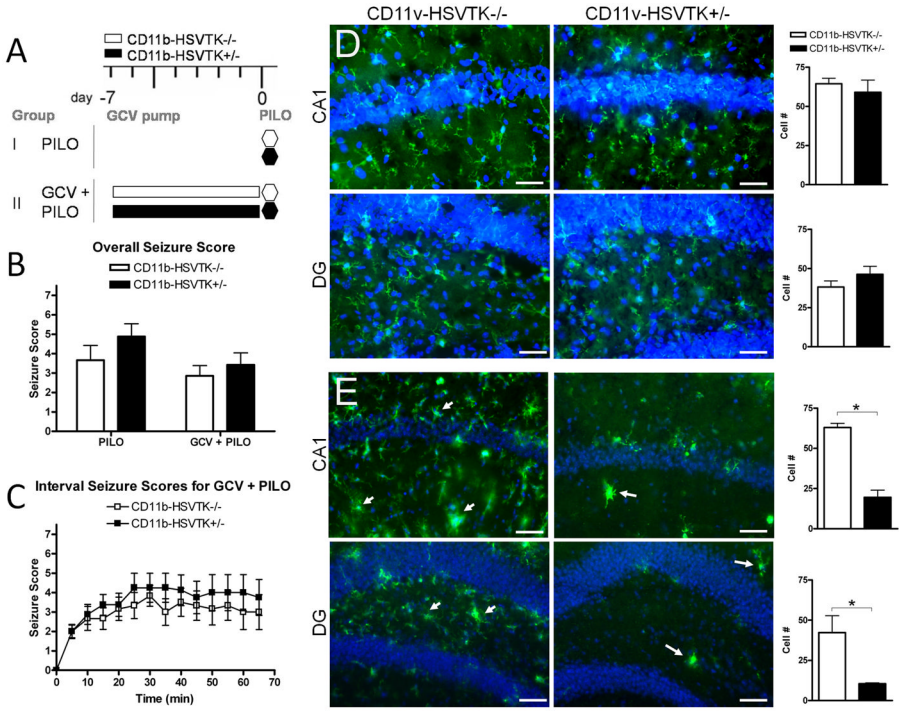

Figure 1. Quiescent hippocampal microglia do not modulate seizure threshold

A) Schematic of experimental design in group I: PILO (pilocarpine only) and II: GCV + PILO (gancyclovir [GCV] infusion before pilocarpine) representing each genotype, white bars are CD11b-HSVK−/− (wild type mice lacking the transgene) and black bars are CD11b-HSVTK +/− (transgenic mice susceptible to microglia ablation by GCV). Administration of pilocarpine (280 mg/kg i.p.) is denoted by a hexagon at day 0 (and is always preceded 15–30 min by methylscopolamine, 2 mg/kg i.p.). Infusion of GCV (for 7 days) is denoted by the rectangular bars from day −7 to 0. B) Following pilocarpine injection, seizure symptoms were continuously recorded, the maximum score during each 5 minute interval was listed over the 60 minute observation period for each animal and averaged by genotype and group providing the overall seizure score. C) The maximum score during each 5 min interval was plotted over time, data points represent the average score ± S.E.M. for each set of animals. D–E) Tissue was collected 2 hours post seizure induction and stained with Iba1 (green fluorescence) for microglia/macrophages. Iba1 is upregulated in activated cells. CA1 and hilar region of the dentate gyrus (DG) are shown with nuclei (DAPI). Panels in D represent group I, and E group II. Arrows in E indicate activated microglia/macrophages. To the right of each set of panels is quantification of Iba1+ cell number counted at 40× in regions of interest (ROIs) sized 300×400μm^2 for each group (scale bar 50 μm, two-way ANOVA, Bonferroni post tests, * = $p<0.05$, data in all graphs plotted as average ± S.E.M.).

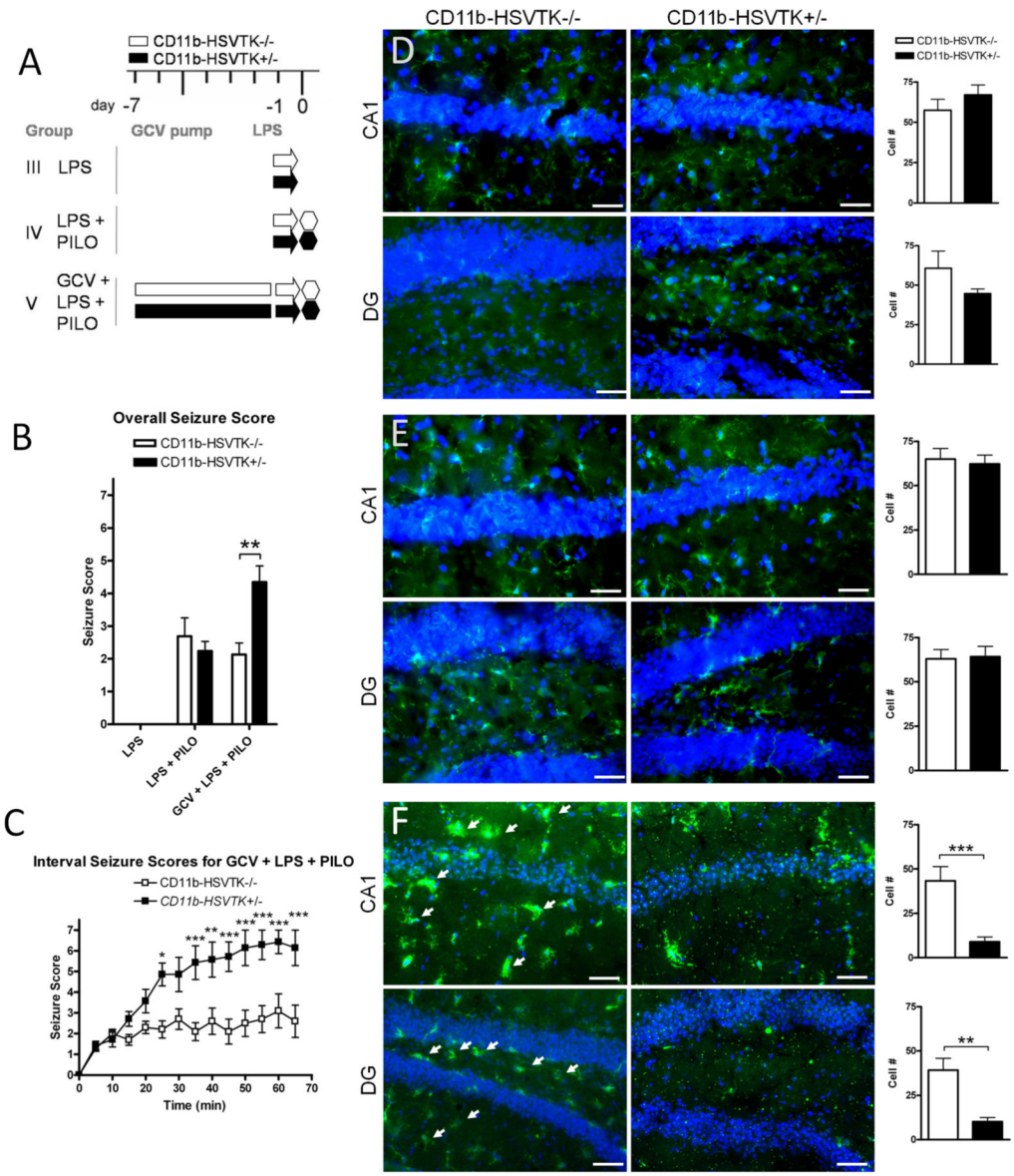

Figure 2. Preconditioning microglia with LPS affects seizure severity differently in CD11b-HSVTK −/− and CD11b-HSVTK+/− mice

A) Schematic of experimental design in group III: LPS (arrows designate lipopolysaccharide [LPS] only, 1 mg/kg i.p.), IV: LPS + PILO (LPS given 24 hours prior to piloarpine [PILO] injection 280 mg/kg i.p.), and V: GCV + LPS + PILO (gancyclovir [GCV] infusion, LPS given at day −1, then pilocarpine given 24 hours later, 280 mg/kg i.p.). Each genotype is represented, white bars for CD11b-HSVK−/− (wild type mice lacking the transgene) and black bars for CD11b-HSVTK+/− (transgenic mice susceptible to microglia ablation by GCV). Administration of pilocarpine is denoted by a hexagon at day 0 (and is always preceded 15–30 min by methylscopolamine, 2 mg/kg i.p.). Infusion of GCV (for 7 days which continues throughout the experiment) is denoted by the rectangular bars from day −7 to 0. B) Following pilocarpine injection, seizure symptoms were continuously recorded; the maximum score during each 5 minute interval was listed over the 60 minute observation period for each animal and averaged by genotype and group providing the overall seizure score. C) The maximum score during each 5 min interval was plotted over time, data points represent the average score

± S.E.M. for each set of animals. D–F) Tissue was collected 2 hours post seizure induction and stained with Iba1 (green fluorescence) for microglia/macrophages. Iba1 is upregulated in activated cells. CA1 and hilar region of the dentate gyrus (DG) are shown with nuclei (DAPI). Panels in D represent group III, E group IV, and F group V. Arrows in F indicate activated microglia/macrophages. The wild type DG panel in F was taken at slightly different coordinates (a more medial aspect of the granule cell layer). To the right of each set of panels is quantification of Iba1+ cell number counted at 40× in regions of interest (ROIs) sized $300\times400\mu m^2$ for each group (scale bar 50 μm, two-way ANOVA, Bonferroni post tests, * = $p<0.05$, ** = $p<0.01$, *** = $p<0.001$, data in all graphs plotted as average ± S.E.M.).

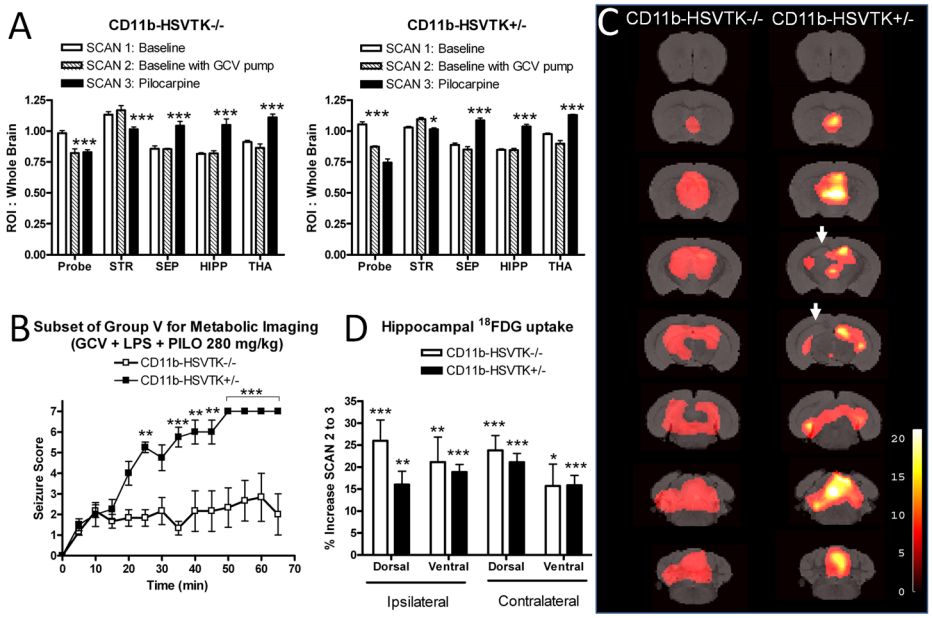

Figure 3. Metabolic correlates of seizures and microglia/macrophages in LPS preconditioned mice

A) A subset of animals from group V were used for serial metabolic imaging experiments (n = 6 CD11b-HSVTK−/− and n = 4 CD11b-HSVTK+/−). Each animal underwent small animal imaging with ^{18}FDG for 3 scans. Scan 1: Baseline, prior to any perturbation (white bars), Scan 2: Baseline with GCV pump, followed implantation with GCV mini pump (hatched bars), San 3: Pilocarpine, regional ^{18}FDG uptake during acute seizures (black bars). ROI analysis developed from a standard template (Ma et al., 2005), with an additional ROI placed at the cortical region above the dorsal hippocampus associated with probe implant (Probe). The graph also shows significant differences in the striatum (STR), septum (SEP), hippocampus (HIPP, left and right combined), and thalamus (THA) for each genotype between scans 1, 2 and 3. B) The maximum score during each 5 min interval was plotted over time, data points represent the average score ± S.E.M. for each subset of animals (**p < 0.01, ***p < 0.001, two-way ANOVA, Bonferroni post-tests to compare replicate means). C) MRI reference template overlaid with voxel based analysis for neuronal activation during acute seizures. Activations in the septum, hippocampus, thalamus, midbrain, and cerebellum are observed. Arrows represent decreased uptake corresponding to the ipsilateral hippocampus. Thresholds for displayed images were set at p < 0.001, uncorrected and *t*-scores are represented by respective color scales. D) Detailed ROI analysis of the hippocampus for CD11b-HSVTK−/− (white bars) and CD11b-HSVTK+/− (black bars), ipsilateral and contralateral to GCV infusion. The percent increase in ^{18}FDG uptake was measured between scan 2 and 3 to correspond to the SPM T-map displayed in ‘C’ (*, p < 0.05, **p<0.01, ***p<0.001, two-tailed *t*-test).

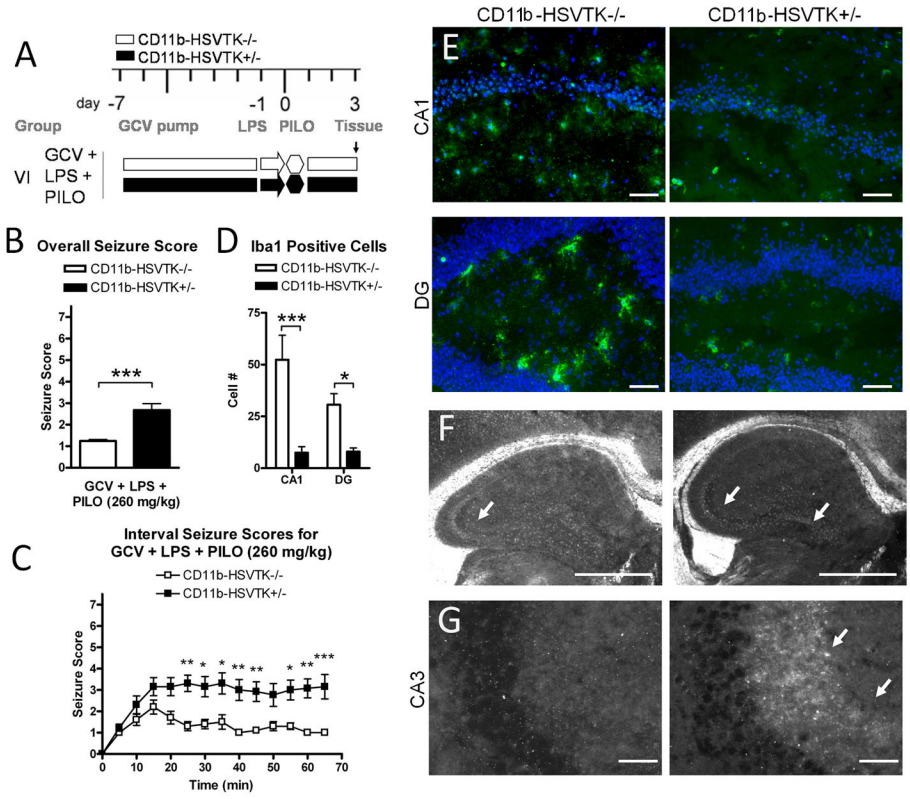

Figure 4. Activated microglia and LPS preconditioning modulate seizure threshold through the mossy fiber pathway

A) Schematic of experimental design in group VI representing ganciclovir (GCV) pump implantation at day −7, LPS pretreatment at day −1, pilocarpine induced seizures at day 0 (260 mg/kg), and tissue collection at day 3, for mice CD11b-HSVTK−/− (white bars) and CD11b-HSVTK+/− (black bars). B) Overall seizure scores were calculated by continuously monitoring acute effects of pilocarpine for 1 hour (the maximum score during 5 min intervals was listed for each animal over 60 minutes, then these twelve scores were averaged together and compared, *t*-test). C) Interval seizure scores are shown for both genotypes, the maximum score during each 5 min interval is plotted over time (Two-way ANOVA, Bonferroni post-tests). D) Quantification of Iba1 positive cells in both genotypes of mice in the CA1 and DG at day 3 (Two-way ANOVA, Bonferroni post-tests). Data in all graphs were plotted as average ± S.E.M., (*, $p < 0.05$, ** $p < 0.01$, *** $p < 0.001$). E) Representative sections of iba1 positive microglia/macrophages (green fluorescence) and nuclei (DAPI, scale bars, 50 μM). F) Zymography analysis for tPA activity following acute seizures, showing tPA activity present in the mossy fiber pathway at day 3 (600 μM scale bar). G) NPY immunoreactivity associated with neurite outgrowth in the CA3 on day 3 of CD11b-HSVTK+/− mice but not −/− (25 μM scale bar).

Table 1

Conditions for experimental groups

Experimental groups	LPS	GCV	Pilocarpine
Group I (3 −/−, 3 +/−)	NO	NO	280 mg/kg
Group II (6 −/−, 8 +/−)	NO	YES	280 mg/kg
Group III (3 −/−, 3 +/−)	YES	NO	NO
Group IV (3 −/−, 3 +/−)	YES	NO	280 mg/kg
Group V (10 −/−, 7 +/−)	YES	YES	280 mg/kg
Group VI (10 −/−, 13 +/−)	YES	YES	260 mg/kg